Biogeosciences Discuss., 8, 12247–12283, 2011
www.biogeosciences-discuss.net/8/12247/2011/
doi:10.5194/bgd-8-12247-2011

Biogeosciences Discussions

^{210}Pb-^{226}Ra chronology reveals rapid growth rate of *Madrepora oculata* and *Lophelia pertusa* on world's largest cold-water coral reef

P. Sabatier[1,2], J.-L. Reyss[3], J. M. Hall-Spencer[4], C. Colin[2], N. Frank[3], N. Tisnérat-Laborde[3], L. Bordier[3], and E. Douville[3]

[1]Université de Savoie, Laboratoire Environnement Dynamiques et Territoire de Montagne, CNRS UMR 5204, 73376 Le Bourget du Lac, France
[2]Université Paris-Sud 11, Laboratoire des Interactions et de la Dynamique des Environnements de Surface, CNRS/INSU UMR 8148, 91405 Orsay, France
[3]Laboratoire des Sciences du Climat et de l'Environnement, UVSQ/CNRS/CEA, UMR 8212, Domaine du CNRS, 91198 Gif/Yvette, France

[4]Marine Biology and Ecology Research Centre, School of Marine Science and Engineering, University of Plymouth, Plymouth, PL4 8AA, UK

Received: 6 December 2011 – Accepted: 7 December 2011 – Published: 21 December 2011

Correspondence to: P. Sabatier (pierre.sabatier@univ-savoie.fr)

Published by Copernicus Publications on behalf of the European Geosciences Union.

BGD
8, 12247–12283, 2011

Abstract

Here we show the use of the ^{210}Pb-^{226}Ra excess method to determine the growth rate of corals from one of the world's largest known cold-water coral reef, the Røst Reef off Norway. Two large branching framework-forming cold-water coral specimens, one *Lophelia pertusa* and one *Madrepora oculata* were collected alive at 350 m water depth from the Røst Reef at ~67° N and ~9° E. Pb and Ra isotopes were measured along the major growth axis of both specimens using low level alpha and gamma spectrometry and the corals trace element compositions were studied using ICP-QMS. Due to the different chemical behaviors of Pb and Ra in the marine environment, ^{210}Pb and ^{226}Ra were not incorporated the same way into the aragonite skeleton of those two cold-water corals. Thus to assess of the growth rates of both specimens we have here taken in consideration the exponential decrease of initially incorporated ^{210}Pb as well as the ingrowth of ^{210}Pb from the decay of ^{226}Ra. Moreover a post-depositional ^{210}Pb incorporation is found in relation to the Mn-Fe coatings that could not be entirely removed from the oldest parts of the skeletons.

The ^{226}Ra activities in both corals were fairly constant, then assuming constant uptake of ^{210}Pb through time the ^{210}Pb-^{226}Ra chronology can be applied to calculate linear growth rate. The 45.5 cm long branch of *M. oculata* reveals an age of 31 yr and a linear growth rate of 14.4 ± 1.1 mm yr^{-1}, i.e. 2.6 polyps per year. However, a correction regarding a remaining post-depositional Mn-Fe oxide coating is needed for the base of the specimen. The corrected age tend to confirm the radiocarbon derived basal age of 40 yr (using ^{14}C bomb peak) with a mean growth rate of 2 polyps yr^{-1}. This rate is similar to the one obtained in Aquaria experiments under optimal growth conditions.

For the 80 cm-long specimen of *L. pertusa* a remaining contamination of metal-oxides is observed for the middle and basal part of the coral skeleton, inhibiting similar accurate age and growth rate estimates. However, the youngest branch was free of Mn enrichment and this 15 cm section reveals a growth rate of 8 mm yr^{-1} (~1 polyp every two to three years). However, the ^{210}Pb growth rate estimate is within the lowermost

BGD
8, 12247–12283, 2011

ranges of previous growth rate estimates and may thus reflect that the coral was not developing at optimal growth conditions.

Overall, ^{210}Pb-^{226}Ra dating can be successfully applied to determine the age and growth rate of framework-forming cold-water corals, however, removal of post-depositional Mn-Fe oxide deposits is a prerequisite. If successful, large branching *M. oculata* and *L. pertusa* coral skeletons provide unique oceanographic archive for studies of intermediate water environmentals with an up to annual time resolution and spanning over many decades.

1 Introduction

The existence of cold-water corals (CWC's) has been known since the 18th century but much less is still known about their ecology and growth patterns compared to their shallow water counterparts (Roberts et al., 2009). Only recently have advances in acoustic survey techniques and the more widespread use of ROVs and submersibles allowed detailed in situ studies of cold-water coral habitats, which revealed a high relief habitat for a number of ecologically important species of invertebrates and fish (Roberts et al., 2009; Soeffker et al., 2011). Today, cold-water coral reefs along the slopes of the Eastern Norwegian Sea are threatened by the deep fishing industry (Hall-Spencer et al., 2009; Clark et al., 2010) and increasing anthropogenic CO_2 emissions are rapidly lowering the aragonite saturation state (Guinotte et al., 2006; Tittensor et al., 2010). Moreover, ocean warming may induce further yet unknown threats. Thus, knowledge about the corals growth rates and regeneration rates is crucial to estimate their capacity to regenerate after reef destruction or to cope with ocean acidification and ocean warming.

Framework forming CWC's are today found in all ocean basins along the margins and topographic heighs within temperature ranges of 4° and 12 °C (~ 50 to 1500 m). Habitat suitability is driven by strong near bottom currents, enhanced labile organic matter fluxes, low sedimentation rates and availability of hard substrata to colonize (Roberts

BGD
8, 12247–12283, 2011

et al., 2009). In addition, CWC's have become unique archives to trace past climate and ocean circulation changes at intermediate and deep depth (Adkins et al., 1998; Magini et al., 1998; Heikoop et al., 2002; Thresher et al., 2004, Frank et al., 2005, van de Flierdt et al., 2006; Colin et al., 2010; Copard et al., 2010). The corals aragonitic skeleton is usually precisely dated by means of ^{230}Th/U and ^{14}C dating (Adkins et al., 1998; Mangini et al., 1998; Cheng et al., 2000; Frank et al., 2004, 2009) and the aragonite skeleton incorporates numerous tracers of water mass provenance, state of ventilation and surface ocean productivity. However, U-series dating and ^{14}C dating is most successful on time scales from decades to thousands of years, but reconstructing the individual growth rate of a single organisms can be done through a large amount of mass spectrometric analyses at very high analytical precision. Alternatively, an age model for recent corals can be established using ^{210}Pb-^{226}Ra methodology as previously shown for various sclerectinian coral species (Moore and Krishnaswami, 1972; Dodge and Thomson, 1974; Druffel et al., 1990; Andrews et al., 2002, 2009; Adkins et al., 2004). These studies used the radioactive decay of ^{210}Pb (half life of 22.3 yr) in excess to its parent, ^{226}Ra, to determine mean growth rates. Other techniques such as counting growth rings (Grigg, 1974) or carbon and oxygen isotopic variations (Fairbanks and Dodge, 1979) in skeleton have been employed to estimate the age of recent coral speciemens. However, for most of those species independent in-situ observations and actual growth rate measurements have not been available to validate the radiometric dating technique and to provide insights on the reproduction cycles.

^{210}Pb-^{226}Ra dating has not been previously applied to the major framework-forming corals *L. pertusa* and *M. oculata* and their skeletal structure with branching and anastonizing coral polyps builds a complex 3-D structure that have proved difficult for sclerochronological analyses (Risk et al., 2005). However, recently these species have provided evidence of strong climate influences on their occurrences (Rüggeberg et al., 2008; Frank et al., 2009, 2011) and their skeletons have been used as an archive to reconstruct water mass provenance in the Eastern North Atlantic (Colin et al. 2010, Copard et al. 2010, 2011). For both species independent growth rate estimates have been

BGD
8, 12247–12283, 2011

obtained from in-situ observations and aquaria studies. Mean growth rate estimates of $26 \pm 5\,\mathrm{mm\,yr^{-1}}$ for *L. pertusa* were made in North Atlantic by measuring the size of colonies reported on oil and gas platforms over time (Bell and Smith, 1999; Gass and Roberts, 2006). Whereas, Orejas et al. (2008), using the bouyant weight technique for specimens maintained in aquaria, found extension rates of 15–17 $\mathrm{mm\,yr^{-1}}$ for *L. pertusa*, and between 3 and 18 $\mathrm{mm\,yr^{-1}}$ for *M. oculata*.

Here we have performed ^{210}Pb-^{226}Ra dating on two framework forming specimens from the world's largest known deep-water coral reef, where corals most likely develop today under optimal growth conditions. The Røst reef has developed in an area along the continental shelf break in the Norwegian Sea. There is growing concern that ocean acidification may hinder growth and encourage dissolution of this reef complex, as the effects of ocean acidification are exacerbated at high latitudes (Maier et al. 2010; Tittensor et al. 2010). Assessing mean growth rate and polyp reproduction rate over recent decades provides a baseline against which to monitor coral growth models as aragonite saturation levels fall and provides independent estimates of recent mean growth rates. Here we evaluate the ^{210}Pb-^{226}Ra dating methodology to establish coral growth models that are then compared to independent growth rate estimates and polyp reproduction cycles. Finally, we discuss some limitations of the ^{210}Pb-^{226}Ra technique for framework-forming CWCs.

2 Corals samples and cleaning

Framework-forming CWC specimens were collected from Rost Reef-complex during the ARK-XX11/1a cruise on the RV Polarstern, using the manned submersible Jago, in June 2007. Røst Reef, discovered in May 2002, is a reef-complex 35–40 km long, up to 3 km wide. It is situated at 300 and 400 m water depth along a steep and rugged part of the continental self break off Norway (Fosså et al., 2005). *L. pertusa* and *M. oculata* corals were collected from an area along the 300–350 m depth contour between 67°30′ N and 67°32′ N; and 9°24′ 30″ E and 9°30′ 30″ E (Fig. 1).

BGD
8, 12247–12283, 2011

The *M. oculata* specimen is 46 cm long and 18 cm wide composed of hundreds of successive coral polyps. Samples were taken for radiometric and trace element analyses along a continuous 45.5 cm branch formed by 80 polyps (Fig. 1). This coral branch was divided perpendicularly to its growth axis into 40 samples of 2 polyps each. The selected branching *L. pertusa* coral is 50 cm long and 20 cm wide and it is again composed of a very large number of individual polyps. It was difficult to sample one continuous section along the entire coral given its complex branching nature. Therefore, three branches with a total length of 80 cm were extracted and sub-divided in 33 samples of 1 polyp each (Fig. 2).

CWC's skeletons that remain exposed to seawater are subject to the post-mortem deposition of ferromanganese oxide and hydroxide coatings (Lomitschka and Mangini 1999; Cheng et al., 2000). Adkins et al. (2004) showed that a cleaning procedure is essential to remove surface contaminant for U-series dating as potential coatings of the coral skeleton contain large amounts of U-series nuclides. In this study, pieces of coral were subsampled by cutting and subjected to rigorous cleaning following the procedure initially presented for U-series dating by Lomitschka and Mangini (1999) and simplified by Copard et al. (2010) to obtain pristine aragonite coral fragments for further geochemical analyses. Briefly, this procedure consists of carefully polishing the inner and outermost surfaces of the coral skeletons using a diamond-bladed saw to remove surface contaminants such as ferromanganese coatings and remains of organic matter. This mechanical cleaning was followed by a weak acid treatment with 0.1 N ultraclean hydrochloric acid in an ultrasonic bath, and the corals were then rinsed several times with Milli-Q water. Cleaned samples were then dried at 54 °C during 2 h, crushed to powder in an agate pestle-mortar and weighed.

In addition, four samples Mb, Mt and Lb, Lt were extracted at the base and the top of the two specimens, but on different branches, M and L, respectively for *M. oculata* and *L. pertusa*. Here, no cleaning was applied to analyse the bulk sample radionuclide composition including the coral's potentially contaminated surface.

BGD
8, 12247–12283, 2011

3 Analytical methods

^{210}Pb, ^{226}Ra, ^{228}Ra, ^{228}Th, ^{234}Th and ^{40}K activities were analyzed on samples using well-type, germanium detectors placed at the Laboratoire Souterrain de Modane (LSM), located under 1700 m of rock. The reduction of crystal background was obtained by the selection of low activity materials and the suppression of the cosmic radiations by placing the detectors in the LSM (Reyss et al., 1995). At the same time, the detector sensitivity allows the reduction of sample mass required for a measurement. These improvements allow measurements of both very low radioactivity levels (with background less than 0.6 pulse per minute for the 30–3000 keV energy range) and low samples volumes (1 g). The ^{226}Ra activities were determined using its short-lived daughters ^{214}Pb (295 keV and 352 keV peaks) and ^{214}Bi (609 keV peak) assuming secular equilibrium with ^{226}Ra. The ^{238}U activities in coral sample were determined through its ^{234}Th daughter peak (63.2 keV). ^{40}K was measured through its gamma emissions at 1460 keV, while ^{228}Th and ^{228}Ra are measured using the gamma-ray emitted by their short-lived descendants: ^{212}Pb (238 keV) and ^{208}Tl (583 keV) for ^{228}Th and ^{228}Ac (338, 911, 970 keV) for ^{228}Ra. The ^{210}Pb (22.3 yr) was directly measured through its gamma emissions at 46.5 keV, but the very low activity of ^{210}Pb does not allow to obtain an accurate estimation with uncertainties of about 30 %. Therefore, ^{210}Pb detection was accomplished by alpha-spectrometry determination of its daughter ^{210}Po (138 d). The extraction was made 2 yr after the collection of the sample to ensuring secular equilibrium with ^{210}Pb. For alpha spectrometric measurements ~ 1 g of cleaned coral of was dissolved in 15 ml of 2 N HCl and 1 ml of 2 % $HClO_4$ and spiked with 1 ml of a 11.8 mBq g^{-1} ^{208}Po solution. The solution was evaporated and then bathed in 1 ml of 2 % $HClO_4$ to fully remove organic matter. The residue was dissolved in 8 N HCl and diluted with Milli-Q water to obtain a 30 ml solution of 0.5 N HCl. The solution was auto-plated onto silver disks at ~ 75 °C for 4 h in the presence of ascorbic acid, following the procedure describe by Flynn (1968). Alpha-spectrometry was performed using grid chamber detectors at the Laboratoire du Climat et de l'Environnement (LSCE) at

BGD
8, 12247–12283, 2011

Gif/Yvette (France). Uncertainties for ^{210}Pb analyses are given as 1 σ uncertainty of counting statistics of samples and blanks. Mn concentrations of corals were analysed on cleaned and dissolved coral fragments using a quadruple ICP-MS Xseries$^{II(Thermo)}$ following the bracketing protocol described by Copard et al. (2010). Samples and standard solutions were systematically adjusted to 100 ppm Ca through dilution. Instrumental calibration based on the standard addition method was achieved using a mono-elementary standard solution. Internal reproducibility for Mn on the JCp-1 standard (100 ppm Ca) was about 5 % (2 σ).

AMS radiocarbon analyses were conducted on five sample aliquots of the *M. oculata* branch of about 10–20 mg size following the procedure published previously (Frank et al., 2004). Samples were converted to CO_2 in a semi-automated carbonate vacuum line (Tisnérat-Laborde et al., 2001), reduced to graphite using hydrogen in the presence of iron powder (Arnold et al. 1989), and measured by the AMS-LMC14 Artemis accelerator facility (Cottereau et al., 2007). They are expressed as pMC normalised to a Δ^{13}C of −25‰ relative to the Pee Dee Belemnite (PDB) international standard according to Stuiver and Polach (1977).

4 ^{226}Ra-^{210}Pb dating method

Since Goldberg (1963) first established a method based on ^{210}Pb chronology, this procedure has provided a very useful tool for dating environmental archives including recently CWC (Adkins et al. 2004). ^{210}Pb precipitates from the atmosphere through ^{222}Rn decay and is scavenged from the surface ocean to deep and intermediate waters where it accumulates on the surface of sediments and corals. In each sample, the ^{210}Pb excess activities were calculated by subtracting the ^{226}Ra activity, derived from the detritic component, from the total (^{210}Pb) activity. In the simplest model, the initial excess of ^{210}Pb activity (^{210}Pb$_{ex}$) is assumed constant and thus (^{210}Pb$_{ex}$) at any time is given by the radioactive decay law (Appleby and Oldfield, 1992). Throughout this

BGD
8, 12247–12283, 2011

paper, parentheses denote activity.

$$\left(^{210}\mathrm{Pb}_{\mathrm{ex}}\right)=\left(^{210}\mathrm{Pb}^{0}_{\mathrm{ex}}\right)e^{-\lambda_{210}t} \quad (1)$$

$$\text{with } \left(^{210}\mathrm{Pb}_{\mathrm{ex}}\right)=\left(^{210}\mathrm{Pb}\right)-\left(^{226}\mathrm{Ra}\right) \quad (2)$$

This $^{210}Pb_{ex}$ method was applied to determine to the growth rate of biogenic carbonates such as marine mollusk shells (Cochran et al., 1981; Turekian and Cochran, 1986) and tropical as well as deep dwelling corals (Moore and Krishnaswami, 1972; Dodge and Thomson, 1974; Druffel et al., 1990; Andrews et al., 2002, 2009; Adkins et al., 2004).

An other method based on ^{210}Pb ingrowth from the ^{226}Ra allow to date young carbonates as nearshore mollusks shells (Baskaran et al., 2005), fish otoliths (Fenton et al., 1991) and whale bones (Schuller et al., 2004). This ^{210}Pb ingrowth method requires either that the initial ^{210}Pb incorporated is negligible compared to the radiogenic ^{210}Pb produced by the decay of ^{226}Ra, or that its initial activity can be estimated. Moreover, the use of this method supposes that the carbonate behaves as a closed system (Baskaran et al., 2005). Thus, ^{210}Pb ingrowth with time is described by the following radioactive decay equation:

$$\left(^{210}\mathrm{Pb}\right)=\frac{\lambda_{210}}{\lambda_{210}-\lambda_{226}}\left(^{226}\mathrm{Ra}\right)\left[1-e^{-(\lambda_{210}-\lambda_{226})t}\right] \quad (3)$$

Since ^{226}Ra has a much longer half-life (1600 yr) than ^{210}Pb (22.3 yr) (or $\lambda_{Pb} \gg \lambda_{Ra}$), this equation is usually written in its simplified form:

$$\left(^{210}\mathrm{Pb}\right)=\left(^{226}\mathrm{Ra}\right)\left[1-e^{-\lambda_{210}t}\right] \quad (4)$$

To date young biogenic carbonates (otoliths, near-shore or deep-sea shells and coral), the use of excess (Eq. 1) or ingrowth (Eq. 4) method mostly depends on the ratio (^{210}Pb/^{226}Ra) of the water in which the organism forms and on the pathways (internal or external organs) by which ions are incorporated into the carbonate (e.g., Schmidt and Cochran, 2010).

BGD
8, 12247–12283, 2011

5 Results

^{210}Pb in "uncleaned" CWC skeletons displayed a very large activities of 72.2 and 161.8 mBq g^{-1} (^{210}Pb) at the base of the two selected coral specimens (M_b for *M. oculata*, L_b for *L. pertusa*), whereas samples from the top (M_t, L_t) show by far less important ^{210}Pb excess of 7.8 and 5.1 mBq g^{-1}, respectively (Table 1 and 2). Thus, the ^{210}Pb composition of uncleaned samples is clearly opposite to the expectation that ^{210}Pb is constantly precipitated as the organisme grows and decays with increasing age of the skeleton. The base of both corals, however, is more affected by post-depositional ferromanganese oxide coatings as dead coral polyps are no longer cleaned by the constant flow of Mucus and therefore post depositional alteration at the sediment water interface is more important. Thus, such disturbances of the corals skeleton composition are clearly documented by a significant post-depositional uptake of ^{210}Pb at the corals skeleton surfaces. In contrast the ^{226}Ra activities was almost constant for all the *M. oculata* sample (clean or not) and for *L. pertusa* the no-cleaning coral present a ^{226}Ra activity slightly higher at the base.

Rigorously cleaned samples from both coral specimens displayed by far weaker ^{210}Pb excess activities (< 6 mBq g^{-1}) and more importantly reveal a decrease or nearly constant ^{210}Pb activities from the top to the base (see Fig. 3). In addition, the ^{226}Ra activities are very similar and can be considered constant within uncertainty with mean values of 1.37 ± 0.05 and 1.60 ± 0.06 mBq g^{-1} for *M. oculata* and *L. pertusa*, respectively. Solely one sample (polyp 12,5) within the *L. pertusa* specimen indicate a minor increase from this mean value (see Fig. 3b). Mn concentrations were also measured on each cleaned sample to indicate the presence of residual ferromanganese oxide hydroxide coatings potentially disturbing ^{210}Pb profiles. Mn concentrations of *M. oculata* (Fig. 3a) are between 0.2 and 2 ppm (5 % of uncertainty), with lowest values at the top (live) polyps and highest values at the base (fossil) polyps. Similarly the topmost *L. pertusa* polpys reveal low Mn contents (around 0.2 ppm) (Fig. 3b), but strongly higher values (between 1.4 and 6.6 ppm) are measured for the middle and basal branchs 2

BGD
8, 12247–12283, 2011

and 3, most likely reflecting a residual Mn-Fe contamination of the skeleton not removed during the cleaning process.

^{210}Pb activities analyzed along the growth axis of *L. pertusa* vary between 6.40 ± 0.34 mBq g^{-1} and 2.99 ± 0.17 mBq g^{-1} and do not reveal a clear decreasing trend along the growth axis as expected from ^{210}Pb decay. However, all (^{210}Pb/^{226}Ra) activity ratios along the coral specimen clearly exceeded secular equilibrium indicating that this *L. pertusa* is propably younger than 100 yr. But, highest ^{210}Pb activities within the middle and basal branches coincide with high residual Mn concentrations and one may thus suspect that both branches contain a significant amount of post-depositional ^{210}Pb as observed far more importantly in the uncleaned samples. For the oldest part of the two last branches of *L. pertusa* a correlation between high Mn content an high ^{210}Pb excess activity is found ($r^2 = 0.83$, $n = 6$) (Fig. 4), whereas such a correlation was absent for the youngest samples of this specimen (blue area). Thus, ^{210}Pb activities in this specimen probably does not reflect the subsequent incorporation and decay throught.

Along the growth axis of *M. oculata* ^{210}Pb activities decrease systematically from 4.80 ± 0.28 mBq g^{-1} (top) to 2.80 ± 0.30 mBq g^{-1} (base). The length of the coral is here expressed in number of polyps from the top, All (^{210}Pb/^{226}Ra) activity ratios along the coral specimen are once more clearly above secular equilibrium indicating that the alive *M. oculata* sampled is again most likely less than a 100 yr old. So (^{210}Pb) data obtained by alpha spectrometry can be used to establish an accurate age model on this deep-sea coral samples. However, in the Fig. 4 the two oldest samples from *M. oculata* specimen seem also perturbed by this Mn contamination (orange area).

BGD
8, 12247–12283, 2011

6 Discussion

6.1 Radionuclide incorporation and implication for ^{226}Ra-^{210}Pb chronology

From ^{226}Ra and ^{210}Pb values described above, two main observations can be made. First, rigorous cleaning is mandatory to eliminate ^{210}Pb added to its surface after the skeleton has formed, whereas this cleaning was apparently not important for ^{226}Ra confirming previous studies on solitary coral species such as *D. dianthus* (Adkins et al., 2004). Second, ^{210}Pb and ^{226}Ra are not incorporated into the CWC skeletons in the same way reflecting the different chemical behavior of radium and lead in the marine environment (Krishnaswami and Cochran, 2008). Lead and its isotopes are readily scavenged onto particles in the water column and have a short oceanic residence time (1 yr in the surface and 30–100 yr in deeper ocean, Cochran et al., 1990) while radium is soluble in seawater and is thus not scavenged onto particules and carbonate surfaces. The source of ^{226}Ra in seawater is essentially diffusion from deep-sea sediments into the overlying bottom water (van Beek and Reyss, 2001). ^{210}Pb inputs to the ocean are mainly atmospheric deposition, where it is produced from ^{222}Rn decay, the in situ production by decay of dissolved ^{226}Ra in seawater and the river-runoff flux of unsupported ^{210}Pb (Appleby and Oldfield, 1992). ^{226}Ra was lattice-bound and not adsorbed within the intercrystaline spaces of the carbonate (Berkman and Ku, 1998) thus, ^{226}Ra is incorporated into carbonate in proportion to their ratio to calcium in seawater (D_{Ra}). In contrast, the geochemical behavior of ^{210}Pb in ocean allows for two incorporation pathways. First lead can be scavenged onto the coral surface where it is trapped during formation of further crystal lattice. Second, ^{210}Pb can be directly incorporated into the crystal lattice from the dissolved state of seawater. Both ^{210}Pb contribution originate from seawater and are further named in this study allochtonous ($^{210}Pb_{all}$). The organisms clean their skeletons from sediments and parasides by a constant flow of mocus along the active skeleton surface. Upon the death of the organisms or an older polyp generation, the flow of mocus stops and the skeleton is thus exposed to seawater without protection leading to the precipitation of secondary authigenic ^{210}Pb

BGD
8, 12247–12283, 2011

accompanied by the production of ferromanganese oxy-hydroxide coatings ($^{210}Pb_{auth}$). This additional ^{210}Pb increases depending on the time of exposure of the coral at the seawater sediment interface, but should be removed during exhaustive cleaning of the coral skeleton (Adkins et al., 2004). Whatever the incorporation mode we can define a ^{210}Pb partition coefficient (D_{Pb}) for the first phase. Therefore, the ($^{210}Pb_{all}/^{226}Ra$) incorporated in deep-sea coral depends on the respective elemental partition coefficient for lead and radium, and the (^{210}Pb)/(^{226}Ra) ratio of the seawater in which the coral growths (Schmidt and Cochran, 2010):

$$\left(\frac{^{210}Pb}{^{226}Ra}\right)_{Carbonate} = \left(\frac{D_{Pb}}{D_{Ra}}\right)\left(\frac{^{210}Pb}{^{226}Ra}\right)_{Water} \quad (5)$$

For CWC's ^{226}Ra is incorporated from seawater and is thus not at secular equilibrium with its radioactive daughter ^{210}Pb. Hence, when ($^{210}Pb_{all}/^{226}Ra$) ratio exceeds 1 the classic used of excess method with initial ^{226}Ra at secular equilibrium with ^{210}Pb can not be applied. Therefore, to describe the temporal variation of ^{210}Pb ($^{210}Pb_t$) we have to take into account either the decrease of ($^{210}Pb_{all}$) initially incorporated to the skeleton and, as suggested by Dodge and Thomson, (1974), the radiogenic ^{210}Pb induce by the ingrowth from ^{226}Ra ($^{210}Pb_{rad}$) (Fig. 5):

$$(^{210}Pb_t) = (^{210}Pb_{rad}) + (^{210}Pb_{all})$$

$$(^{210}Pb_t) = \underbrace{(^{226}Ra_t)\left[1 - e^{-\lambda_{210}t}\right]}_{\text{Ingrowth}} + \underbrace{(^{210}Pb_0)e^{-\lambda_{210}t}}_{\text{Decrease}}$$

$$(^{210}Pb_t) = (^{226}Ra_t) + \left(^{210}Pb_0 - ^{226}Ra_t\right)e^{-\lambda_{210}t} \quad (6)$$

If the studied system was closed and if initial ^{210}Pb ($^{210}Pb_0$) is further assumed constant, this equation allows to date any young carbonate using the ^{210}Pb-^{226}Ra chronology, whatever is the incorporation mode of these radioelements. Therefore, the growth

BGD
8, 12247–12283, 2011

rate (V) was defined by the best fit of the ^{210}Pb data by the Eq. (6), with $V = z/t$, whereas z is the distance from the base of the coral (express in mm or number of polyps). However, it was shown that ($^{226}Ra_t$) is constant through time, hence Eq. (6) can be simplified:

$$\left(^{210}\text{Pb}-^{226}\text{Ra}\right)_t = \left(^{210}\text{Pb}-^{226}\text{Ra}\right)_0 \times e^{-\lambda_{210}t} \quad (7)$$

Knowing Eq. (2), this last equation (Eq. 7) can be described by the excess model (Eq. 1) and the growth rate of the CWC can be estimated through the following equation:

$$\ln\left(^{210}\text{Pb}^{t}_{ex}\right) = \ln\left(^{210}\text{Pb}^{0}_{ex}\right) - \lambda_{210} \times \frac{z}{V} \quad (8)$$

6.2 Estimated coral growth rates

The excess of (^{210}Pb) data (Fig. 6) displays a well-constrained slope for the *M. oculata* specimen providing evidence that the uptake of initial ($^{210}Pb_{ex}$) occurs at a nearly constant rate. The low Mn concentrations (Fig. 3) associated to the well-constrained slope (Fig. 6) apparently indicate that the cleaning procedure applied here was successful to remove authigenic radionucleides from the skeleton surface. The exponential slope for $^{210}Pb_{ex}$ corresponds to a linear growth rate of 2.58 ± 0.19 polyp yr^{-1} or 14.4 ± 1.1 mm yr^{-1}. This growth rate estimate yields an basal age of 31 ± 3 yr ($1\,\sigma$) for this 45 cm-long specimen of *M. oculata*. The age determined using Eq. (7) instead of Eq. (8), thus, assuming a variable flux of (^{226}Ra) yields the same results within uncertainties. Moreover, with the presently available and limited data (7 measures of (^{210}Pb) regularly distributed along the branch) there is no indication of a growth interruption for this coral specimen, as no significant offset is observed between each data point Andrews et al. (2009). To validate this age model, five independent ^{14}C analysis were performed along the *M. oculata* specimen (Table 3). They show an increase of ^{14}C data between the base and the top of the coral of 99.1 pM C until 105.6 pM C. This increase indicate that the coral recorded a part of the ^{14}C nuclear bomb produced during the

BGD
8, 12247–12283, 2011

era of atmospheric testing. The pre-bomb value in intermediate waters in 1950 can be estimated lower than 93 pM C if we consider that $\Delta^{14}C$ of intermediare waters are still around −70‰ as suggested by previous studies (Frank et al., 2004; Sherwood et al., 2008). Therefore, we can consider that *M. oculata* coral has less than 60 yr old. In order to better constrain the age scale, we compared these ^{14}C data with ^{14}C data of the dissolved inorganic carbon in seawater which are collected nearby the location of the coral during different oceanographic cruise; GEOSECS (1972, Ostlund et al., 1974), TTO cruise (1981, Broecker et al., 1985) and Norwegian research cruise (1990, Nydal et al., 1992). The ^{14}C comparison yields an age estimate between 37 and 43 yr for this specimen (Fig. 7). Thus age deduced from bomb-^{14}C is here 40 ± 3 yr corresponding to a linear growth rates of 2 polyps yr^{-1} or 11.2 cm yr^{-1}. At 2σ uncertainty levels both bomb-^{14}C and ^{210}Pb-^{226}Ra age estimates are almost identical. The slightly younger age estimate obtained from ^{210}Pbex may reflect the progressive increase of Mn contamination towards the base of the organism leading to an overestimation of ^{210}Pbex values at the corals base (Fig. 6) mainly for the two last samples identified as Mn contaminated in the Fig. 4.

In contrast, the more complex *L. pertusa* specimen presents high ^{228}Th activities with respect to the decay of its parent isotope ^{228}Ra. The half-life of ^{228}Th is 1.91 yr, thus for the oldest samples (> 10 yr) the $^{228}Th/^{228}Ra$ activity ratio must be at secular equilibrium in a closed system. These ^{228}Th excess activities imply that this system was submitted to post-growth deposition of radionuclides, not removed by the cleaning, which probably affect the ^{210}Pb-^{226}Ra chronology.

Moreover, the elevated Mn contents in particular of the older branchs of specimen (B2 and B3) reveal also a high degree of residual skeleton contamination with ferromanganese oxide/hydroxide coatings that could apparently not be fully removed during the cleaning. Yet we have no reasonable explanation for this as the cleaning protocol has been often applied to *L. pertusa* corals with excellent results regarding the removal of such coatings (Copard et al., 2010). However if we exclude the most contaminated samples (high ^{228}Th activities and high Mn concentrations, especially for

BGD
8, 12247–12283, 2011

branch 3) it is possible to estimate a linear growth rate of 0.34 and 0.32 polyp yr^{-1} for the branches 1 and 3, respectively (Fig. 8). This values would correspond to a growth rate of about 8 mm yr^{-1} and would provide a time of 18 yr covered by the more recent branch (B1). However, these estimations imply a different uptake of initial (^{210}Pbex) for both branches. Both growth rate estimates are in good agreement but as solely few points are incorporated in the model and given the additional hypothesis of a variable initial (^{210}Pbex) this result does not seem confident. Moreover, difficulties appear to extract a continuous section along this coral in relation to its growth complexity (Brooke and Young, 2009), thus this cold -water coral genus appears presently (1) difficult to date by ^{226}Ra-^{210}Pb chronology and (2) it is less evident to provide a continuous record of environmental conditions.

6.3 Impact of metal oxide coatings and Mn corrections

As described in result section, a correlation ($r^2 = 0.83$) is here present between Mn content and level of ^{210}Pb excess for the two older branch B2 and B3 of *L. pertusa* specimen (Figure 4). The first growth rate estimation of *M. oculata* (2.58 ± 0.19 polyp yr^{-1}) was probably impacted by Mn contamination on the two oldest samples (Fig. 4). Thus, to overcome this influence a Mn correction for the radionuclides can be proposed. As a simple assumption, we estimate an additional ^{210}Pb contribution based on the measured ^{210}Pbex/Mn ratio on *L. persuta* to correct the two older ^{210}Pbex values on *M. oculata*. This correction presumes that the ^{210}Pb excess associated to ^{210}Pb-^{226}Ra data would be negligible for the oldest parts of *L. pertusa* compared to $^{210}Pb_{oxide}$ and secondly the $^{210}Pb_{oxide}$/Mn ratio is presumed constant through time. Such a correction model bring back the two last samples to a Mn content equivalent to the other part of the *M. oculata* coral (bleu area in Fig. 4) and allow to correct these two ^{210}Pbex values from the $^{210}Pb_{oxide}$. Applying this simple model to the *M. oculata* specimen, which only at its base shows slightly elevated Mn concentrations yields an growth rate of 1.6 ± 0.3 polyp yr^{-1} and an age of 42–61 yr ($r^2$0.85, $n = 7$). Thus the correction yields

BGD
8, 12247–12283, 2011

an increase of the coral age, however it older than the estimated ^{14}C age of 40 yr. This indicates that the ^{210}Pb excess substracted by the Mn correction, is evidently too strong as based on the ^{14}C ages. However, for this correction we do not taking account the $^{210}Pb_{oxide}$ decay after its coating, which itself occurred between the basal age of the coral and the sampling date. Thus the $^{210}Pb_{oxide}$ /Mn ratio must be lower than first estimated (Fig. 4), but without any information about the timing of the coating on each samples we can not made a right correction, highlighting that an advanced cleaning procedure is a key issue to precisely date coral sample with ^{210}Pb-^{226}Ra method. However, even if the Mn correction remain uncertain due to the lack of information about the processes and the period of formation of metal-enriched phases, the age estimation gives a minimum growth rate of this sample (1.6 ± 0.3 polyp yr^{-1}), while the first estimation without any correction gives a maximum growth rate of this *M. oculata* specimen (2.58 ± 0.19 polyp yr^{-1}). These results tend to confirm the ^{14}C estimation with a mean growth rate for this *M. oculata* about 2 polyp yr^{-1} and an age close to 40 yr old.

This type of correction can not be applied on the *L. pertusa* specimen in relation to the very high Mn content of the two last branch (B2 and B3).

6.4 Coral growth rate comparison

For the *M. oculata* coral, only a few growth rate estimates are reported in the literature with values ranging from as low as 3 mm yr^{-1} to as high as 18 mm yr^{-1} with a maximum addition of 5 polyp yr^{-1}, obtained in aquaria (Orejas et al., 2008). The linear growth rate calculated for *M. oculata* is made on one single branch and therefore can not be simply compared to that obtained by Orejas et al. (2008) because in this study the number of polyps were not defined along one and unique axis.

Overall our growth rate estimates (around 2 polyps yr^{-1} or 11.2 cm yr^{-1}) best agree with the highest rates observed in aquaria and from in-situ observation in the Nordic Seas. The northern most reefs of *L. pertusa* and *M. oculata* are amongst the most

BGD
8, 12247–12283, 2011

active reefs known today, with sizes of individual colonies that exceed several meters of height and thus comprising thousands of individual coral generations.

Therefore our present work brings new information about the maximum in situ linear growth rate and polyp regeneration rate of *M. oculata*. Our findings further highlight that a branching cold-water coral comprising several polyp generations, here 80, reflect the formation of aragonite skeleton over several decades, potentially allowing the reconstruction of physical and chemical properties of subsurface seawater at high latitude with a resolution of close to 1 yr.

Growth rate estimation of $26 \pm 5\,\mathrm{mm\,yr^{-1}}$ for *L. pertusa* were made in the North Atlantic by measuring the size of colonies reported on oil and gas platforms over time (Bell and Smith, 1999; Gass and Roberts, 2006). Studies using stable isotopes estimated corallites grow of *L. pertusa* from 5 to $10\,\mathrm{mm\,yr^{-1}}$ (Mortensen and Rapp, 1998) and U-series measurements gave a mean growth rates between 2.2 and $5.0\,\mathrm{mm\,yr^{-1}}$ (Pons-Branchu et al., 2005). Using coral fragments maintained in aquaria Orejas et al. (2008) found extension rates of 15–17 $\mathrm{mm\,yr^{-1}}$ for *L. pertusa* while Brooke and Young (2009), with in situ experiment estimate this rate to 2–4 $\mathrm{mm\,yr^{-1}}$. Brooke and Young, (2009) explained this discrepancies between the documented linear growth rates for this specie by the maturity difference of the polyps with a value $> 16\,\mathrm{mm\,yr^{-1}}$ and $< 5\,\mathrm{mm\,yr^{-1}}$ for new and more mature polyps, respectively. The *L. pertusa* investigated in this study is characterized by a growth rate ($0.33\,\mathrm{polyp\,yr^{-1}}$ or $8\,\mathrm{mm\,yr^{-1}}$) in accordance with the range of previously reported data. Therefore, we found that *M. oculata* was easier to work with than *L. pertusa* when providing continuous oceanographic archives to study hydrological changes with a yearly temporal resolution. However, *L. pertusa* may well be dated using a more riguours cleaning and implying a more complex sampling selection strategy based on the tangled growth of the successives poly generations.

BGD
8, 12247–12283, 2011

7 Conclusions

^{226}Ra-^{210}Pb chronology was applied in this study for the first time to large branching specimens of *L. pertusa* and *M. oculata*, two constructional deep-sea scleractinian corals which form large deep-sea reefs that are of great ecological and conservation importance in the North Atlantic. ^{210}Pb and ^{226}Ra were not incorporated the same way into the deep-sea corals in relation to different chemical behaviors in the aquatic environment. Pb isotopes readily scavenge onto particles, whereas Ra isotopes are soluble in seawater. To describe the temporal variation of ^{210}Pb, we have to take into account the decrease of ^{210}Pb initially incorporated to the skeleton ($^{210}Pb_{all}$) and, the ingrowth of ^{210}Pb from skeleton bound ^{226}Ra ($^{210}Pb_{rad}$). Since ^{226}Ra activities in both deep-sea corals were fairly constant, a constant uptake of ^{210}Pb with time was assumed and thus the ^{210}Pb-^{226}Ra chronology was applied to calculate linear growth rate expressed in mm per year or polpyp generations per year.

For the specimen of *M. oculata*, a linear growth rate was initially calculated at 2.6 ± 0.2 polyp yr^{-1} or 14.4 ± 1.1 mm yr^{-1} with an age of 31 yr obtained for the oldest polyp of this colonial deep-sea coral sepcimeny. However, the reltivelly high Mn content for the last samples reveals a post deposition of $^{210}Pb_{oxide}$that induced an overestimation of the growth rate. A Mn correction was applied to these samples and a minimum growth rate was calculated at 1.6 ± 0.3 polyp yr^{-1}. But this simple correction do not taking account the $^{210}Pb_{oxide}$ decay after its coating and gives a minimum growth rate estimation. These results tend to confirm the ^{14}C estimation with a mean growth rate for this *M. oculata* about 2 polyp yr^{-1} and an age close to 40 yr old. Moreover the age model indicates a continuous growth of this *M. oculata* specimen during all the period covered here. For the *L. pertusa*, Mn concentrations revealed a high level of contamination of metal/radionuclide-oxides especially for the oldest parts of the coral, except for the upper branch of 15 cm where a linear growth rate could be estimated at 0.33 polyp yr^{-1} or 8 mm yr^{-1}, however with an important uncertainty. The strong presence of Mn-rich phases and the complexity of the *L. pertusa* growth, with frequent

BGD
8, 12247–12283, 2011

recrutement of coral polyps on older specimens, thus prevented accurate growth rate estimated for this very important colonial species. In conclusion ^{226}Ra-^{210}Pb method applied to deep-sea corals can provide continuous well dated oceanographic archives over the last several decades with a less than 1 yr resolution to study intermediate or deep seawater environmental parameters. But to further apply ^{226}Ra-^{210}Pb method to the major reef-building corals like *M. oculata* or *L. pertusa*, need to be free of Mn/Fe coatings or an advanced cleaning protocol has to be inevitably developed.

Acknowledgements. Sincere thanks to the IFM-GEOMAR Jago submersible team together with crew and scientists aboard RV Polarstern during the Alfred Wegener Institute coordinated cruise ARK-XXII/1a. This work was part-funded by the EC-funded Framework 7 projects Knowledge-based Sustainable Management for Europe's Seas (KnowSeas grant agreement number 226675) and contributes to the European Project on Ocean Acidification (EPOCA grant agreement number 211384).

References

Adkins, J. F., Cheng, H., Boyle, E. A., Druffel, E. R. M., and Edwards, R. L.: Deep-sea coral evidence for rapid change in ventilation of the deep North Atlantic 15 400 years ago, 9 Science, 280, 725–728, 1998.

Adkins, J. F., Henderson, G. M., Wang, S.-L., O'Shea, S., and Mokadem, F.: Growth rates of the deep-sea scleractinia *Desmophyllum cristagalli* and *Enallopsammia rostrata*, Earth Planet. Sc. Lett., 227, 481–490, 2004.

Andrews, A. H., Cordes, E., Mahoney, M. M., Munk, K., Coale, K. H., Cailliet, G. M., and Heifetz, J.: Age and growth and radiometric age validation of a deep-sea, habitat-forming gorgonian (*Primnoa resedaeformis*) from the Gulf of Alaska, Hydrobiologia, 471, 101–110, 2002.

Andrews, A. H., Stone, R. P., Lundstrom, C. C., and DeVogelaere, A. P.: Growth rate and age determination of bamboo corals from the Northeastern Pacific Ocean using refined ^{210}Pb dating, Mar. Ecol.-Prog. Ser., 397, 173–185, 2009.

Appleby, P. and Oldfield, F.: Chapter Application of Lead-210 to Sedimentation Studies, in:

BGD

8, 12247–12283, 2011

Uranium Series Disequilibrium, Application to Earth, Marine and Environmental Sciences, edited by: Ivanovich, M. and Harmon, R. S., Clarendon Press, Oxford, 731–778, 1992.
Arnold, M., Bard, E., Maurice, P., Valladas, H., and Duplessy, J.-C.: ^{14}C dating with the Gif-sur-Yvette Tandetron accelerator: status report and study of isotopic fractionation in the sputter ion source, Radiocarbon, 31, 284–91, 1989.
Baskaran, M., Hong, G.-H., Kim, S.-H., and Wardle, W. J.: Reconstructing seawater column ^{90}Sr based upon ^{210}Pb/^{226}Ra disequilibrium dating of mollusc shells, Appl. Geochem., 20, 1965–1973, 2005.
van Beek, P. and Reyss, J. L.: ^{226}Ra in marine barite: new constraints on supported ^{226}Ra, Earth Planet. Sc. Lett., 33, 147–161, 2001.
Bell, B. and Smith, J.: Coral growing on North Sea oil rigs, Nature, 402, 601, 1999.
Berkman, P. A. and Ku, T.-L.: ^{226}Ra/Ba ratios for dating Holocene biogenic carbonates in the Southern Ocean: preliminary evidences from Antarctic coastal mollusk shells, Chem. Geol., 144, 331–334, 1998.
Broecker, W. S., Peng, T.-H., Ostlund, H. G., and Stuiver, M.: The distribution of bomb radiocarbon in the ocean, J. Geophys. Res., 90, 6925–6939, 1985.
Brooke, S. and Young, C. M.: In situ measurement of survival and growth of *Lophelia pertusa* in the Northern Gulf of Mexico, Mar. Ecol.-Prog. Ser., 397, 153–161, 2009.
Cheng, H., Adkins, J. F., Edwards, R. L., and Boyle, E. A.: U-Th dating of deep-sea corals, Geochim. Cosmochim. Ac., 64, 2401–2416, 2000.
Clark, M. R., Rowden, A. A., Schlacher, T., Williams, A., Consalvey, M., Stocks, K. I., Rogers, A. D., O'Hara, T. D., White, M., Shank, T. M., and Hall-Spencer, J. M.: The ecology of seamounts: structure, function and human impacts, Annu. Rev. Mar. Sci., 2, 253–278, 2010.
Cochran, J. K., Rye, D. M., and Landman, N. H.: Growth rate and habitat of *Nautilus pompilius* inferred from radioactive and stable isotope studies, Paleobiology, 7, 469–480, 1981.
Cochran, J. K., McKibbin-Vaughan, T., Dornblaser, M. M., Hirschberg, D., Livingston, H. D., and Buesseler, K. O.: ^{210}Pb scavenging in the North Atlantic and North Pacific Oceans, Earth Planet. Sc. Lett., 97, 332–352, 1990.
Colin, C., Frank, N., Copard, K., and Douville, E.: Neodymium isotopic composition of deep-sea corals from the NE Atlantic: implications for past hydrological changes during the Holocene, Quaternary Sci. Rev., 29, 2509–2517, 2010.
Copard, K., Colin, C., Douville, E., Freiwald, A., Gudmunsson, G., de Mol, B., and Frank, N.: Nd

BGD
8, 12247–12283, 2011

isotopes in deep-sea corals in the North-Eastern Atlantic, Quaternary Sci. Rev., 29, 2499–2508, 2010.
Copard, K., Colin, C., Frank, N., Jeandel, C., Montero-Serrano, J.-C., Reverdin, G., and Ferron, B.: Nd isotopic composition of water masses and dilution of the Mediterranean outflow along the Southwest European margin, Geochem. Geophy. Geosy., 12, Q06020, doi:10.1029/2011GC003529, 2011.
Cottereau, E., Arnold, M., Moreau, C., Baqué, D., Bavay, D., Caffy, I., Comby, C., Dumoulin, J.-P., Hain, S., Perron, M., Salomon, J., and Setti, V.: Artemis, the new ^{14}C AMS at LMC14 in Saclay, France, Radiocarbon, 49, 291–299, 2007.
Dodge, R. E. and Thomson, J.: The natural radiochemical and growth records in contemporary hermatypic corals from the Atlantic and Caribbean, Earth Planet. Sc. Lett., 23, 313–322, 1974.
Druffel, E. R. M., King, L. L., Belastock, R. A., and Buesseler, K. O.: Growth rate of a deepsea coral using ^{210}Pb and other isotopes, Geochim. Cosmochim. Ac., 54, 1493–1500, 1990.
Fairbanks, R. G. and Dodge, R. E.: Annual periodicity of the 18O/16O and 13C/12C ratios in the coral *Montastrea annularis*, Geochim. Cosmochim. Ac., 43, 1009–1020, 1979.
Fenton, G. E., Short, S. A., and Ritz, D. A.: Age determination of orange roughy, *Hoplostethus atlanticus* (*Pisces*: *Trachichthyidae*) using ^{210}Pb:^{226}Ra disequilibria, Mar. Biol., 109, 197–202, 1991.
van de Flierdt, T., Robinson, L. F., Adkins, J. F., Hemming, S. R., and Goldstein, S. L.: Temporal stability of the neodymium isotope signature of the Holocene to glacial North Atlantic, Paleoceanography, 21, 1–6, 2006.
Flynn, W. W.: The determination of low levels of polonium-210 in environmental samples, Anal. Chim. Acta, 43, 221–227, 1968.
Fosså, J. H., Lindberg, B., Christensen, O., Lundalv, T., Svellingen, I., Mortensen, P., and Alvsvag, J.: Mapping of Lophelia reefs in Norway: experiences and survey methods, in: Cold-water Corals and Ecosystems, edited by: Freiwald, A. and Roberts, J. M., Springer-Verlag, Berlin-Heidelberg, Germany, 337–370, 2005.
Frank, N., Paterne, M., Ayliffe, L., van Weering, T., Henriet, J. P., and Blamart, D.: Eastern North Atlantic deep-sea corals: tracing upper intermediate water Δ^{14}C during the Holocene, Earth Planet. Sc. Lett., 219, 297–309, 2004.
Frank, N., Lutringer, A., Paterne, M., Blamart, D., Henriet, J. P., Van Rooij, D., and Van Werinng, T.: Deepwater corals of the Northeastern Atlantic margin: carbonate mound evolu-

BGD
8, 12247–12283, 2011

tion and upper intermediate water ventilation water ventilation during the Holocene, in: Cold Water Corals and Ecosystems, edited by: Freiwald, A. and Roberts, J. M., Springer-Verlag, Berlin-Heidelberg, Germany, 113–133, 2005.

Frank, N., Ricard, E., Lutringer-Paquet, A., van der Land, C., Colin, C., Blamart, D., Foubert, A., Van Rooij, D., Henriet, J. P., de Haas, H., and van Weering, T.: The Holocene occurrence of cold water corals in the NE Atlantic: implications for coral carbonate mound evolution, Mar. Geol., 266, 129–142, 2009.

Freiwald, A., Fosså, J. H., Grehan, A., Koslow, T., and Roberts, J. M.: Cold-Water Coral Reefs, UNEP-WCMC, Cambridge, UK, 86 pp., 2004.

Gass, S. E. and Roberts, M.: The occurrence of the cold-water coral *Lophelia pertusa* (Scleractinian) on oil and gas plateforms in the North Sea: colony growth, recruitment and environmental controls on distribution, Mar. Pollut. Bull., 52, 549–559, 2006.

Golberg, E.: Radioactive dating, in: Geochronology with Lead-210, edited by: Internationale Atomic Energy Agency, International Atomic Energy Agency, Vienna, Austria, 121–131, 1963.

Grigg, R. W.: Growth rings: annual periodicity in two gorgonian coral, Ecology, 55, 876–881, 1974.

Guinotte, J. M., Orr, J., Cairns, S., Freiwald, A., Morgan, L., and George, R.: Will human-induced changes in seawater chemistry alter the distribution of deep-sea scleractinian corals?, Front. Ecol. Environ., 4, 141–146, 2006.

Hall-Spencer, J. M., Tasker, M., Soffker, M., Christiansen, S., Rogers, S., Campbell, M., and Hoydal, K.: The design of marine protected areas on high seas and territorial waters of Rockall, Mar. Ecol.-Prog. Ser., 397, 305–308, 2009.

Heikoop, J. M., Hickmott, D. D., Risk, M. J., Shearer, C. K., and Atudorei, V.: Potential climate signal from the deep-sea gorgonian coral *Primnoa resedaeformis*, Hydrobiology, 471, 117–124, 2002.

Krishnaswami, S. and Cochran, J. K.: Radioactivity in the environment, in: U–Th Series Nuclides in Aquatic Systems, 13, edited by : Krishnaswami, S. and Cochran, J. K., Elsevier, New York, 458 pp., 2008.

Lomitschka, M. and Mangini, A.: Precise Th/U-dating of small and heavily coated samples of deep sea corals, Earth Planet. Sc. Lett., 170, 391–401, 1999.

Maier, C., Hegeman, J., Weinbauer, M. G., and Gattuso, J.-P.: Calcification of the cold-water coral *Lophelia pertusa*, under ambient and reduced pH, Biogeosciences, 6, 1671–1680,

BGD
8, 12247–12283, 2011

doi:10.5194/bg-6-1671-2009, 2009.
Mangini, A., Lomitschka, M., Eichstädter, R., Frank, N., Vogler, S., Bonani, G., Hajdas, I., and Pätzold, J.: Coral provides way to age deep water, Nature, 392, 347, 1998.
Moore, W. S. and Krishnaswami, S.: Coral growth rates using Ra-228 and Pb-210, Earth Planet. Sc. Lett., 15, 187–190, 1972.
Mortensen, P. B. and Rapp, H. T.: Oxygen and carbon isotope ratios related to growth line patterns in skeletons of *Lophelia pertusa* (L.) (*Anthozoa*: *Scleractinia*): implications for determination of linear extension rates, Sarsia, 83, 433–446, 1998.
Mortensen, P. B., Hovland, M., Brattegard, T., and Farestveit, R.: Deep-water bioherms of the scleractinian coral *Lophelia pertusa* (L.) at 64 N on the Norwegian shelf: structure and associated megafauna, Sarsia, 80, 145–158, 1995.
Nydal, R., Gislefoss, J., Skjelvan, I., Skogseth, F., Jull, A. J. T., and Donahue, D. J.: ^{14}C profiles in the Norwegian and Greenland Seas by conventional and AMS measurements, Radiocarbon, 34, 717–726, 1992.
Orejas, C., Gori, A., and Gili, J. M.: Growth rates of live *Lophelia pertusa* and *Madrepora oculata* from the Mediterranean Sea maintained in aquaria, Coral Reefs, 27, 255, 2008.
Ostlund, H. G., Dorsey, H. G., and Rooth, C. G.: GEOSECS North Atlantic radiocarbon and tritium results, Earth Planet. Sc. Lett., 23, 69–86, 1974.
Pons-Branchu, E., Hillaire-Marcel, C., Deschamps, P., Ghaleb, B., and Sinclair, D. J.: Early diagenesis impact on precise U-series dating of deep-sea corals: example of a 100–200-year old *Lophelia pertusa* sample from the Northeast Atlantic, Geochim. Cosmochim. Ac., 69, 4865–4879, 2005.
Reyss, J.-L., Schmidt, S., Legeleux, F., and Bonté, P.: Large, low background well-type detectors for measurements of environmental radioactivity, Nucl. Instrum. Meth. A, 357, 391–397, 1995.
Risk, M., Hall-Spencer, J. M., and Williams, B.: Climate records from the Faroe-Shetland Channel using *Lophelia pertusa* (Linnaeus, 1758), in: Cold Water Corals and Ecosystems, edited by: Freiwald, A. and Roberts, J. M., Springer-Verlag, Berlin-Heidelberg, Germany, 2005.
Roberts, J. M., Brown, C. J., Long, D., and Bates, C. R.: Acoustic mapping using a multibeam echosounder reveals coldwater coral reefs and surrounding habitats, Coral Reefs, 24, 654, 2005.
Roberts, J. M., Wheeler, A., Friewald, A., and Cairns, S.: Cold-Water Corals the Biology and Geology of Deep-Sea Coral Habitats, Cambridge University Press, 334 pp., Cambridge,

BGD
8, 12247–12283, 2011

2009.
Rüggeberg, A., Fietzke, J., Liebetrau, V., Eisenhauer, A., Dullo, W.-C., and Freiwald, A.: Stable strontium isotopes (d88/86Sr) in cold-water corals – a new proxy for reconstruction of intermediate ocean water temperatures, Earth Planet. Sc. Lett., 269, 570–575, 2008.
Schmidt, S. and Cochran, J. K.: Radium and radium-daughter nuclides in carbonates: a briefs overview of strategies for determining chronologies, J. Environ. Radioactiv., 101, 530–537, 2010.
Schuller, D., Kadko, D., and Smith, C. R.: Use of ^{210}Pb/^{226}Ra disequilibria in the dating of deep-sea whale falls, Earth Planet. Sc. Lett., 218, 277–289, 2004.
Sherwood, O. A., Edinger, E. N., Guilderson, T. P., Ghaleb, B., Risk, M. J., and Scott, D. B.: Late Holocene radiocarbon variability in Northwest Atlantic slope waters, Earth Planet. Sc. Lett., 275, 146–153, 2008.
Söffker, M., Sloman, K. A., and Hall-Spencer, J. M.: In situ observations of fish associated with coral reefs off Ireland, Deep-Sea Res. Pt. I, 58, 818–825, 2011.
Stuiver, M. and Polach, H. A.: Discussion reporting of ^{14}C data, Radiocarbon, 19, 355–363, 1977.
Thresher, R., Rintoul, S. R., Koslow, C., Weidman, C., Adkins, J., and Proctor, C.: Oceanic evidence of climate change in Southern Australia over the last three centuries, Geophys. Res. Lett., 31, LO7212, doi:10.1029/2003GL018869, 2004.
Tisnérat-Laborde, N., Poupeau, J.-J., Tannau, J.-F. and Paterne, M.: Development of a semi-automated system for routine preparation of carbonate sample, Radiocarbon, 43, 299–304, 2001.
Tittensor, D. P., Baco, A. R., Hall-Spencer, J. M., Orr, J. C., and Rogers, A. D.: Seamounts as refugia from ocean acidification for cold-water stony corals, Mar. Ecol.-Prog. Ser., 31, 212–225, 2010.
Turekian, K. K. and Cochran, J. K.: Flow rates and reaction rates in the Galapagos Rise spreading center hydrothermal system as inferred from ^{228}Ra/^{226}Ra in vesicomyid clam shells, P. Natl. Acad. Sci. USA, 83, 6241–6244, 1986.

BGD
8, 12247–12283, 2011

Table 1. Radiometric data from the *Madrepora oculata* specimen, activity was determined as milli-Becquerel per gram ($mBq\,g^{-1}$) with standard deviation at $1\,\sigma$. In bold, data obtained by gamma spectrometry with activities of ^{210}Pb, ^{226}Ra, ^{238}U, ^{228}Th, ^{228}Ra and ^{40}K. In regular, ^{210}Pb activities obtained by alpha spectrometry.

Polyps	Mass (g)	^{210}Pb ($mBq\,g^{-1}$)	^{226}Ra ($mBq\,g^{-1}$)	^{238}U ($mBq\,g^{-1}$)	^{228}Th ($mBq\,g^{-1}$)	^{228}Ra ($mBq\,g^{-1}$)	^{40}K ($mBq\,g^{-1}$)
2	**1.453**	**3.8 ± 1.1**	**1.57 ± 0.13**	**48 ± 2.7**	**0.37 ± 0.05**	**0.09 ± 0.03**	**0.48 ± 0.07**
1	0.971	4.8 ± 0.28					
14	**1.97**	**4.4 ± 1**	**1.34 ± 0.11**	**41 ± 2**	**0.28 ± 0.05**		**0.25 ± 0.03**
12	0.936	4.58 ± 0.31					
27	0.995	3.81 ± 0.24					
35	**2.15**	**4.1 ± 0.8**	**1.29 ± 0.1**	**37 ± 2**	**0.25 ± 0.04**		**0.22 ± 0.03**
35	1.135	3.59 ± 0.19					
51	**2.041**	**4.5 ± 0.9**	**1.41 ± 0.11**	**42 ± 2**			**0.22 ± 0.03**
51	0.987	3.45 ± 0.18					
66	**2.13**	**3.9 ± 0.9**	**1.28 ± 0.1**	**41 ± 2**	**0.26 ± 0.04**	**0.2 ± 0.08**	**0.23 ± 0.03**
68	0.994	2.83 ± 0.15					
76	**2.21**	**2.9 ± 0.8**	**1.39 ± 0.1**	**38 ± 2**	**0.31 ± 0.05**	**0.19 ± 0.08**	**0.13 ± 0.03**
77	0.987	2.8 ± 0.3					
Mt	**1.72**	**7.8 ± 1.0**	**1.93 ± 0.10**	**47 ± 2**	**0.22 ± 0.02**	**0.26 ± 0.06**	**0.35 ± 0.04**
Mb	**2.07**	**72.2 ± 4.4**	**1.96 ± 0.21**	**49 ± 4**	**2.09 ± 0.2**	**0.19 ± 0.12**	**0.47 ± 0.09**

BGD
8, 12247–12283, 2011

Table 2. Radiometric data from the *Lophelia pertusa* specimen, activity was determined as milli-Becquerel per gram ($mBq\,g^{-1}$) with standard deviation at $1\,\sigma$. In bold, data obtained by gamma spectrometry with activities of ^{210}Pb, ^{226}Ra, ^{238}U, ^{228}Th, ^{228}Ra and ^{40}K. In regular, ^{210}Pb activities obtained by alpha spectrometry. Some samples are below the limit of detection (/).

Polyps	Mass (g)	^{210}Pb ($mBq\,g^{-1}$)	^{226}Ra ($mBq\,g^{-1}$)	^{238}U($mBq\,g^{-1}$)	^{228}Th ($mBq\,g^{-1}$)	^{228}Ra ($mBq\,g^{-1}$)	^{40}K ($mBq\,g^{-1}$)
0.5	0.71	4.04 ± 0.28					
5	**2.045**	**2.9 ± 0.9**	**1.69 ± 0.11**	**33 ± 2**	**0.5 ± 0.05**	**0.09 ± 0.03**	**0.53 ± 0.07**
4.5	0.87	3.72 ± 0.34					
5.5	1.177	3.04 ± 0.34					
12.5	**1.02**	**5.9 ± 1.4**	**2.13 ± 0.16**	**37 ± 3**	**2.7 ± 0.17**	**0.5 ± 0.13**	**0.53 ± 0.07**
9	0.51	5.52 ± 0.26					
16	0.5	5.28 ± 0.25					
21	**2.12**	**2.3 ± 1**	**1.68 ± 0.12**	**36 ± 2**	**0.39 ± 0.05**	**0.25 ± 0.07**	**0.35 ± 0.05**
20.5	1.1	5.27 ± 0.18					
26.5	**1.3**	**5.6 ± 1.2**	**1.39 ± 0.12**	**39 ± 2.5**	**1.31 ± 0.1**	**0.09 ± 0.04**	**0.42 ± 0.05**
26	0.68	6.4 ± 0.34					
27.5	0.62	6 ± 0.34					
31	**1.74**	**3.9 ± 0.9**	**1.65 ± 0.11**	**36 ± 2**	**0.05 ± 1**	**/ ± /**	**0.39 ± 0.05**
31	1.74	2.99 ± 0.17					
Lt	**1.79**	**5.1 ± 1.3**	**1.89 ± 0.16**	**35 ± 2**	**0.27 ± 0.06**	**0.25 ± 0.12**	**0.60 ± 0.01**
Lbc	**1.19**	**3 ± 1.8**	**1.63 ± 0.18**	**36 ± 3**			
Lb	**4.68**	**161.8 ± 2.1**	**2.95 ± 0.09**	**36 ± 1**	**2.37 ± 0.07**	**0.71 ± 0.1**	**1.40 ± 0.10**

BGD
8, 12247–12283, 2011

Table 3. Radiocarbon data from the *Madrepora oculata* specimen and from dissolved inorganic carbon of water collected nearby the area of coral growth. In bold is noted the radiocarbon data expressed as pM C. The lower and upper limit of growth year was estimated by adjusting the data of *M. oculata* and those of seawater considering a linear growth.

Seawater Cruise ID	Station	Latitude	Longitude	Depth (m)	**pM C**	**err pM C**	Year	Reference
GEOSECS Atlantic	Station 19	64.2° N	5.6° W	247	**104.4**	**0.3**	1972	Oslund et al. (1974)
				349	**104.1**	**0.3**		
				458	**103.1**	**0.3**		
				558	**102.8**	**0.3**		
TTO	Station 144	67.7° N	3.3° W	448	**104.9**	**0.3**	1981	Broecker et al. (1985)
	Station 145	70.0° N	2.5° E	449	**105.2**	**0.3**		
Norwegian research vessels	GS 19	69.9° N	9.7° E	400	**105.3**	**0.4**	1990	Nydal et al. (1992)

Madrepora oculata Sample ID	Measurement ID	Latitude	Longitude	Depth (m)	**pM C**	**err pM C**	$Year_{lowerlimit}$(37 yr)	$Year_{upperlimit}$(43 yr)
Mad 79	GifA 09467 - SacA 17521	67.5° N	9.4–9.5° E	300–350	**99.1**	**0.3**	1970	1964
Mad 75	GifA 09472 - SacA 17526	67.5° N	9.4–9.5° E	300–350	**104.1**	**0.3**	1974	1968
Mad 52	GifA 09481 - SacA 17535	67.5° N	9.4–9.5° E	300–350	**105.0**	**0.4**	1982	1978
Mad 32	GifA 09487 - SacA 17541	67.5° N	9.4–9.5° E	300–350	**105.2**	**0.3**	1992	1989
Mad 2	GifA 09496 - SacA 17673	67.5° N	9.4–9.5° E	300–350	**105.6**	**0.3**	2006	2006

BGD
8, 12247–12283, 2011

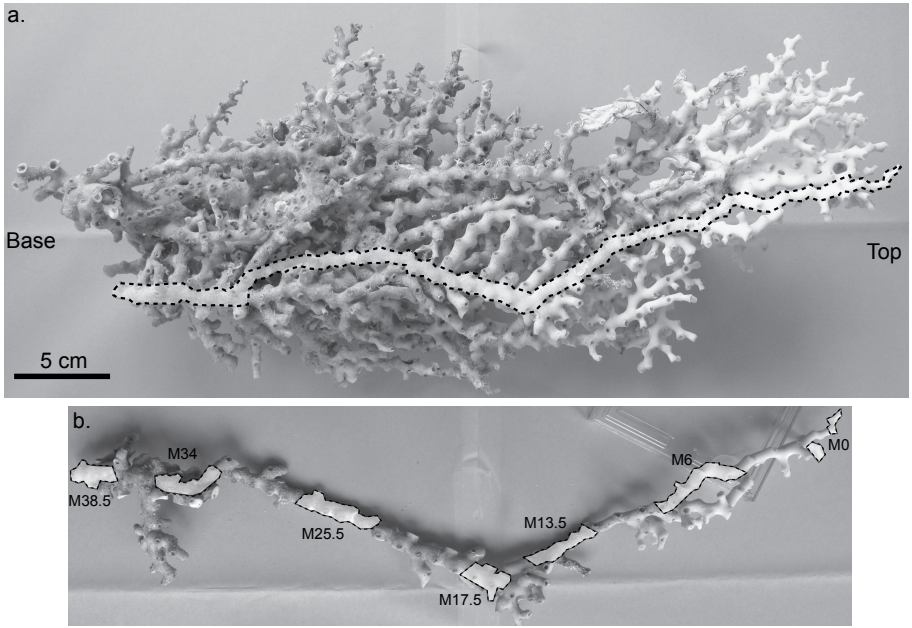

Fig. 1. Subsampling of *Madrepora oculata* specimen. **(a)** Extraction of a continuous branch along the coral, **(b)** location of samples analyzed for ^{226}Ra-^{210}Pb chronology.

BGD
8, 12247–12283, 2011

^{210}Pb-^{226}Ra chronology of cold-water corals

P. Sabatier et al.

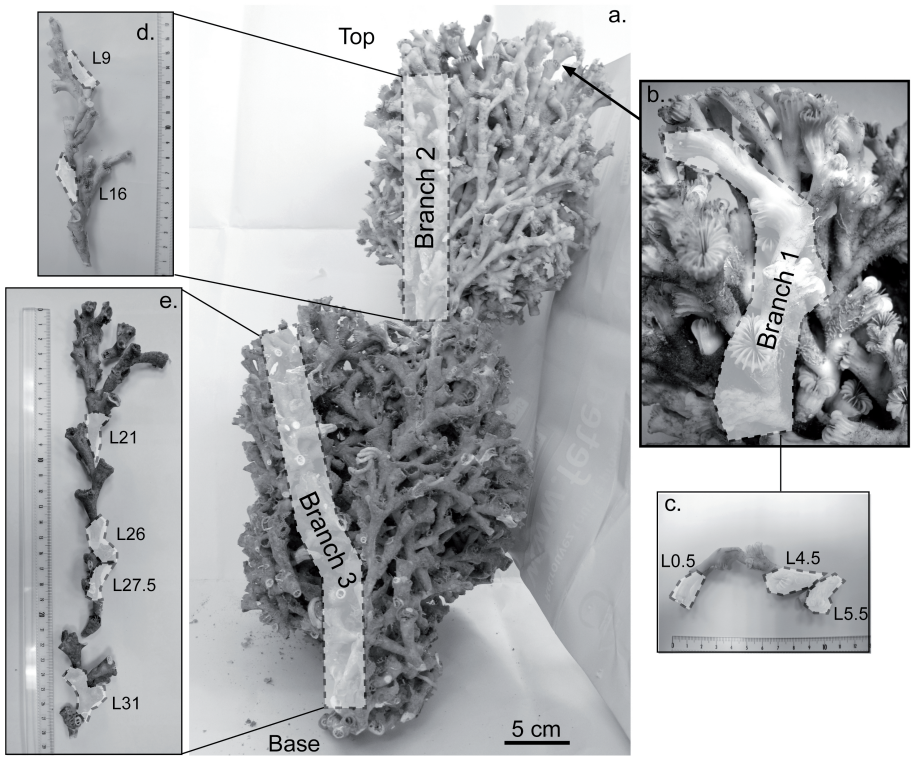

Fig. 2. (a) Photograph of *Lophelia pertusa* specimen with the identification of branch 2 and 3, **(b)** location and identification of branch 1 in the upper part of the coral. Location of samples analyzed for ^{226}Ra-^{210}Pb chronology on extracted branch 1 **(c)**, branch 2 **(d)**, and branch 3 **(e)**.

BGD
8, 12247–12283, 2011

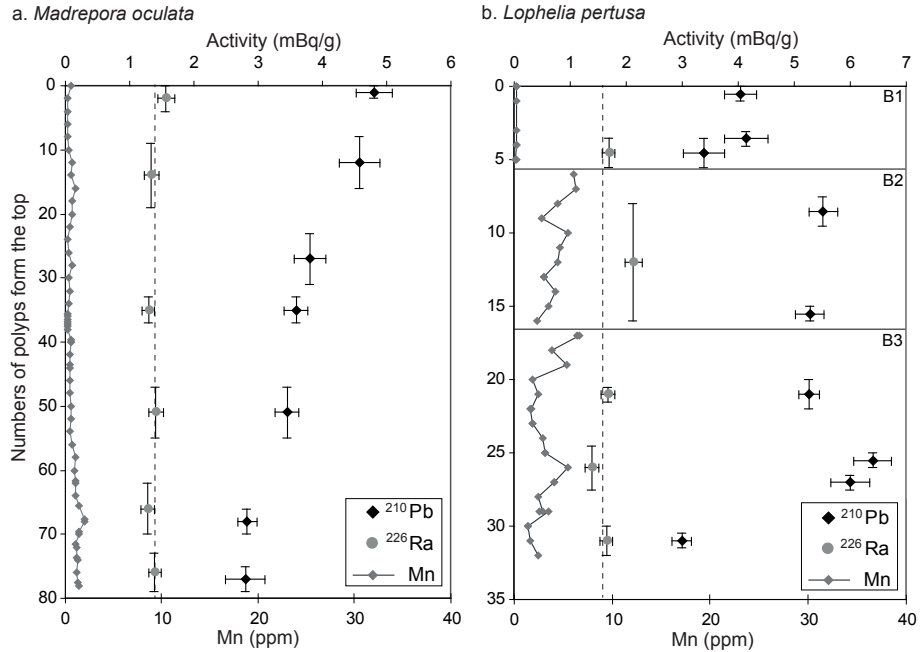

Fig. 3. ^{210}Pb activities (black dots), ^{226}Ra activities (grey dots) and Mn content (grey curve) from mechanically and chemically cleaned polyps of *Madrepora oculata* **(a)** and *Lophelia pertusa* **(b)** specimen. Dotted line displays the mean activity of ^{226}Ra. Horizontal dotted lines represent the limit of the three sampled branches of *Lophelia pertusa* (B1, B2, and B3).

BGD
8, 12247–12283, 2011

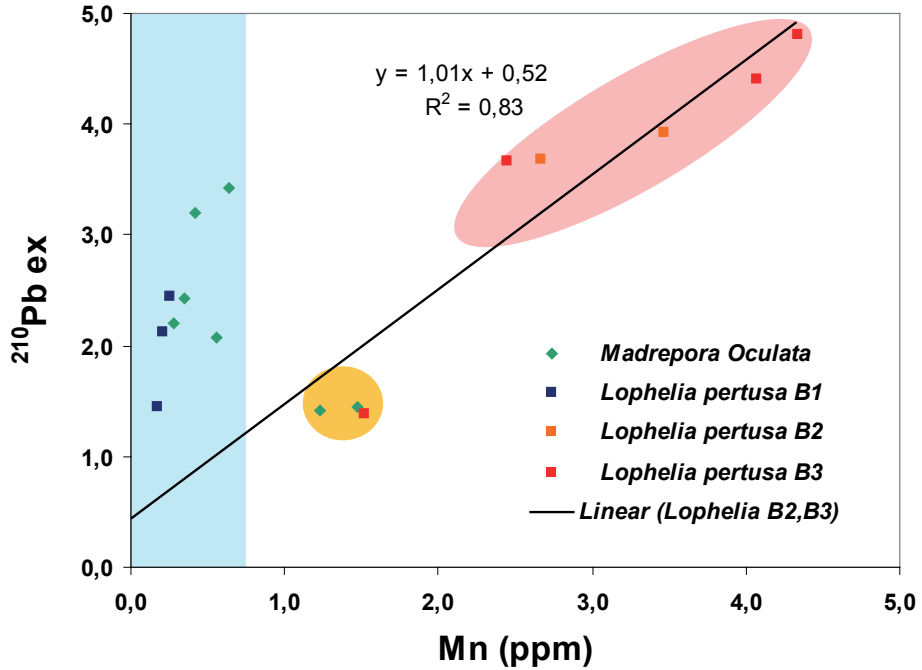

Fig. 4. ^{210}Pb excess versus Mn concentrations for the two *Madrepora oculata* and *Lophelia pertusa* specimens studied here. This graph reveals a marked link between the presence of Mn-oxydes and the level of ^{210}Pb excess for the older parts of each coral fragments. Such effect strongly limits to use of the ^{210}Pb-^{226}Ra method for older Mn-rich deep-sea corals. Red, orange and bleue area represent, respectively highly, moderate and low Mn-contamined coral samples.

BGD
8, 12247–12283, 2011

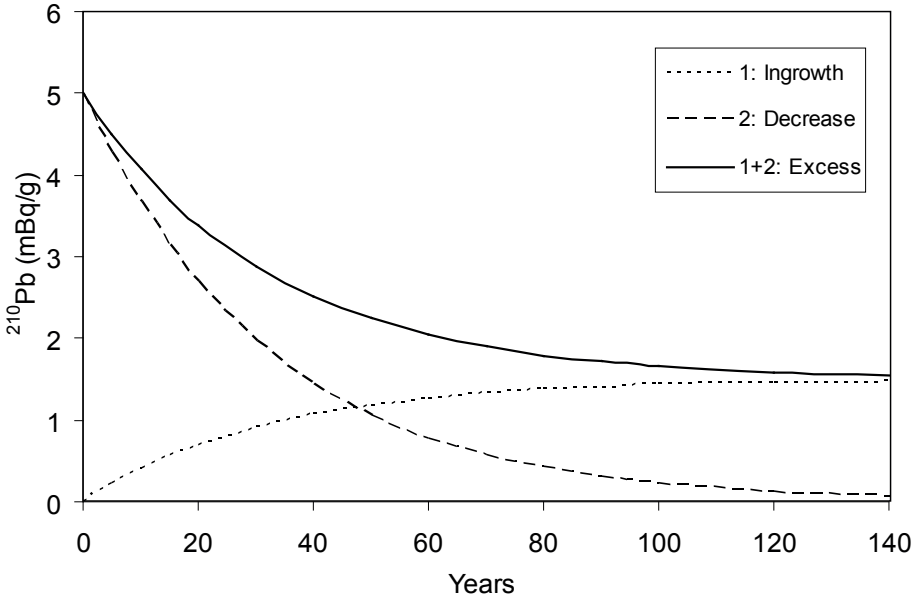

Fig. 5. Theoretical evolution of ^{210}Pb activity as a function of time for the decrease (1), ingrowth (2) and excess model (3). Excess model is the sum of decrease and ingrowth patterns.

BGD
8, 12247–12283, 2011

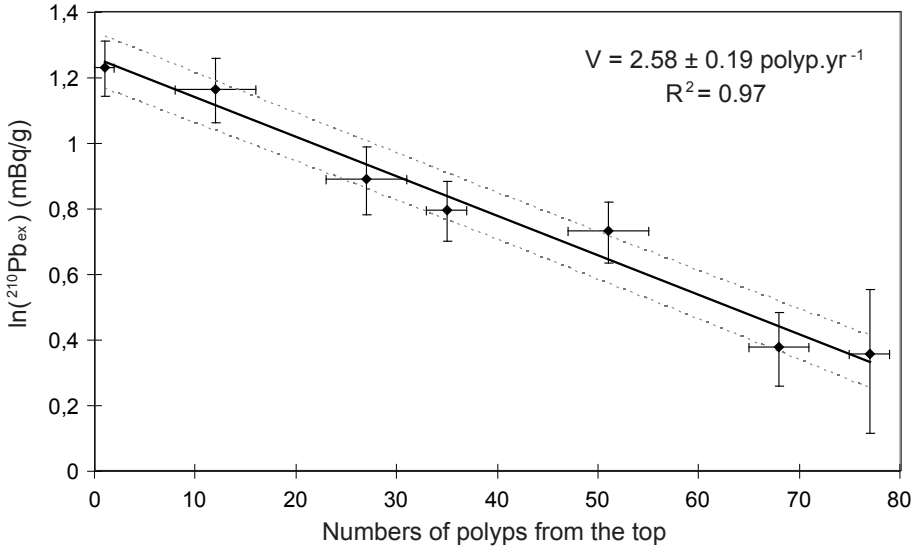

Fig. 6. ln-transformation of ^{210}Pb excess relative to the number of polyps from the top of the *Madrepora oculata* specimen. The slope of this linear regression revealed a linear growth rate of 2.58 ± 0.19 polyp yr^{-1}.

BGD
8, 12247–12283, 2011

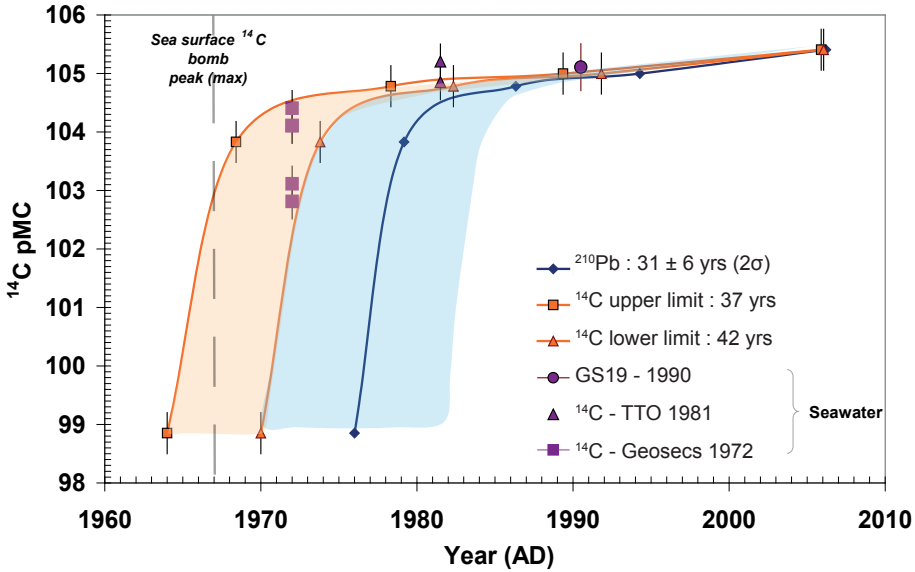

Fig. 7. Age model comparison for the *Madrepora oculata* specimen. Coral ^{14}C measurements expressed as pM C compared to available seawater ^{14}C data of dissolved inorganic carbon (see text GEOSECS, TTO and Norwegian research cruise) allow to identify the bomb ^{14}C peak with an age for the base of between 37 and 43 yr. This estimation is in agreement at 2 σ with that of ^{210}Pb-^{226}Ra method. The dashed line indicate the year of sea surface ^{14}C bomb maximum.

BGD
8, 12247–12283, 2011

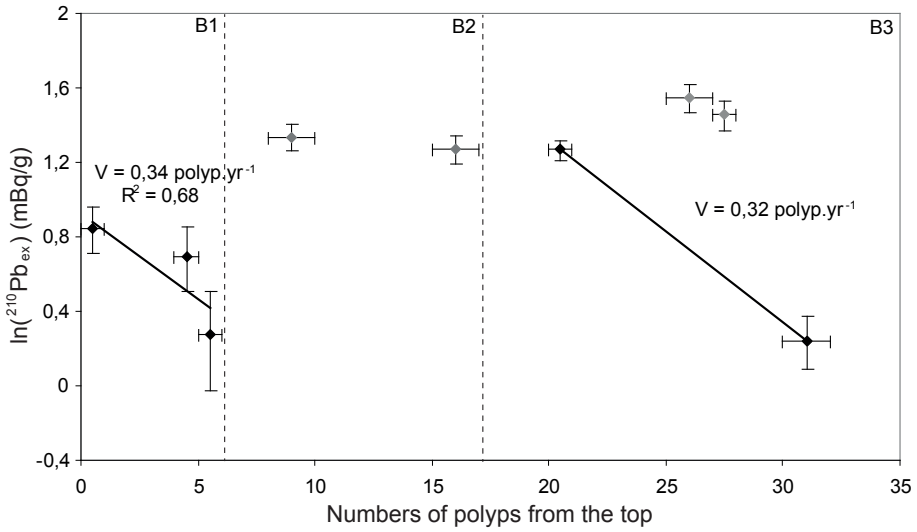

Fig. 8. ln-transformation of ^{210}Pb excess relative to the number of polyps from the top of the *Lophelia pertusa* specimen. Grey points presented high ^{228}Th activities and Mn content that were not included in the linear regression. The slope of these two linear regressions revealed a linear growth rate between 0.34 and 0.32 polyp yr^{-1} with an large uncertainty in relation to few points considered here. Horizontal dotted lines represent the limit of the three sampled branches (B1, B2, B3).

BGD
8, 12247–12283, 2011